NEMO DOUBLE-BETA-DECAY EXPERIMENTS *)

A.S. BARABASH

Institute of Theoretical and Experimental Physics,
B. Cheremushkinskaya 25, 117259 Moscow, Russia

for NEMO Collaboration**)

Received 6 August 1997

To investigate double beta decay processes the NEMO collaboration developed an electron tracking detector made of Geiger cells for track reconstruction and plastic scintillators for energy measurements. The prototype, NEMO-2, is described and results on $\beta\beta$ decay of ^{100}Mo, ^{116}Cd, ^{82}Se and ^{96}Zr are given. A brief presentation of the status and design parameters of a new detector NEMO-3, which is approximately 20 times larger, will also be given.

1 Introduction

The NEMO collaboration is building the NEMO-3 [1] detector for double beta decay experiments which will be capable of studying $\beta\beta0\nu$ decays of ^{100}Mo and other nuclei with half-lives up to $\approx 10^{25}$ y corresponding to neutrino masses of 0.1 to 0.3 eV. Two prototype detectors, NEMO-1 [2] and NEMO-2 [3], have been constructed as research and development efforts to establish reliable techniques. NEMO-2 is currently operating in the Fréjus Underground Laboratory (4800 m.w.e.). Presented here are the final results for ^{100}Mo and ^{116}Cd, the preliminary results for ^{82}Se and ^{96}Zr, and the present status of the detector NEMO-3.

2 NEMO-2 detector and $\beta\beta$ decay experiments with ^{100}Mo, ^{116}Cd, ^{82}Se and ^{96}Zr

2.1 NEMO-2 detector

NEMO-2 [3] consists of a 1 m^3 tracking volume filled with helium gas and 4% ethyl alcohol (Fig. 1). Vertically bisecting the detector is the plane of the source foil (1×1 m^2). The tracking portion of the detector is made of open Geiger cells with octagonal cross sections defined by 100 μm nickel wires. These cells are identical to those of NEMO-1 and work in the Geiger mode. On each side of the source there are 10 planes of 32 cells which alternate between vertical and horizontal orientations. The cells provide three-dimensional tracking of charged particles by recording the drift time and two plasma propagation times in each cell.

*) Presented by A.S. Barabash at the Workshop on calculation of double-beta-decay matrix elements (MEDEX'97), Prague, May 27–31, 1997.

**) CEN-Bordeaux-Gradignan, France; CFR-Gif/Yvette, France; CRN-Strasbourg, France; Department of Physics-Jyväskylä, Finland; FNSPE-Prague, Czech Republic; INEL-Idaho Falls, USA; INR-Kiev, Ukraine; ITEP-Moscow, Russia; JINR-Dubna, Russia; LAL-Orsay, France; LPC-Caen, France; MHC-South Hadley, USA.

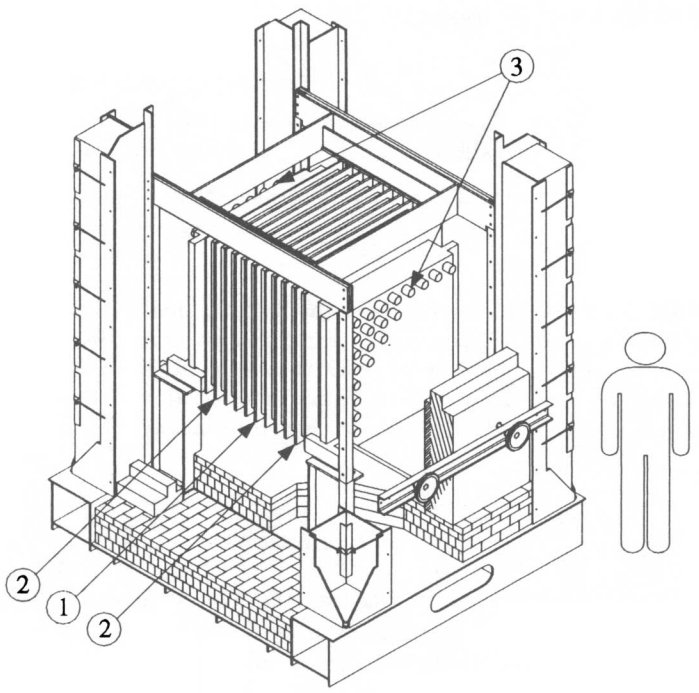

Fig. 1. The NEMO-2 detector. (1) Central frame with the metallic foil. (2) Tracking device of 10 frames with 2 × 32 Geiger cells each. (3) Scintillator array. (The shielding is not shown.)

A calorimeter made of scintillators covers two opposing, vertical sides of the tracking volume. Two configurations of the calorimeter have been implemented. The first one consisted of 2 planes of 64 scintillators ($12 \times 12 \times 2.25\,\mathrm{cm}^3$) associated with "standard" photomultiplier tubes (PMTs). This configuration was used in the experiment with ^{100}Mo. The present configuration includes 2 planes of 25 scintillators ($19 \times 19 \times 10\,\mathrm{cm}^3$) with PMTs made of low radioactive glass. The tracking volume and scintillators are surrounded by a lead (5 cm) and iron (20 cm) shield.

The performance and operating parameters are as follows. The threshold for the scintillators is set at 50 keV, the energy resolution (FWHM) is 18% at 1 MeV and the time resolution is 275 ps for a 1 MeV electron (550 ps at 0.2 MeV). In the 2e event analysis an electron is defined by a track linking the source foil and a scintillator with an energy deposited in the

scintillator(s) greater than 200 keV. The maximum scattering angle along the track has to be less than 20° to reject hard scattering situations. Electrons crossing the detector are rejected by time-of-flight analysis. Finally, the NEMO-2 detector is able to measure the internal radioactive contamination of the foils by using the electron-gamma ($e\gamma$) and electron-gamma-alpha ($e\gamma\alpha$) channels.

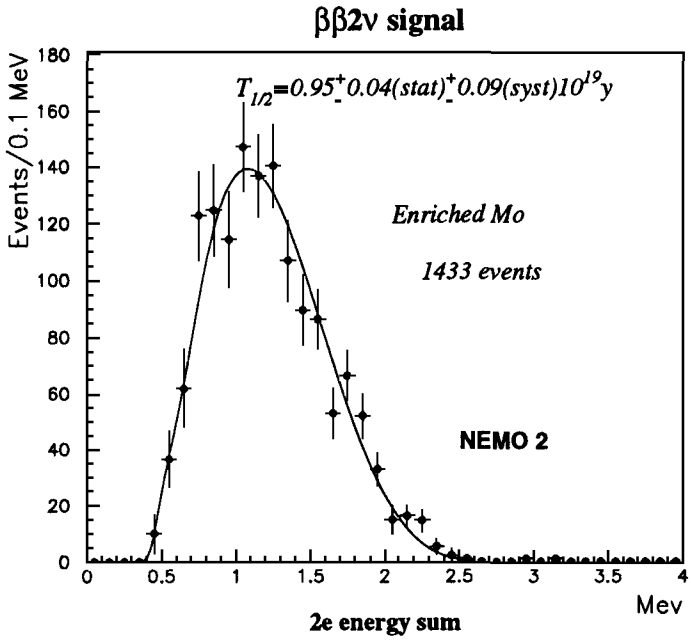

Fig. 2. Summed electron energy spectrum of $\beta\beta2\nu$ events in ^{100}Mo.

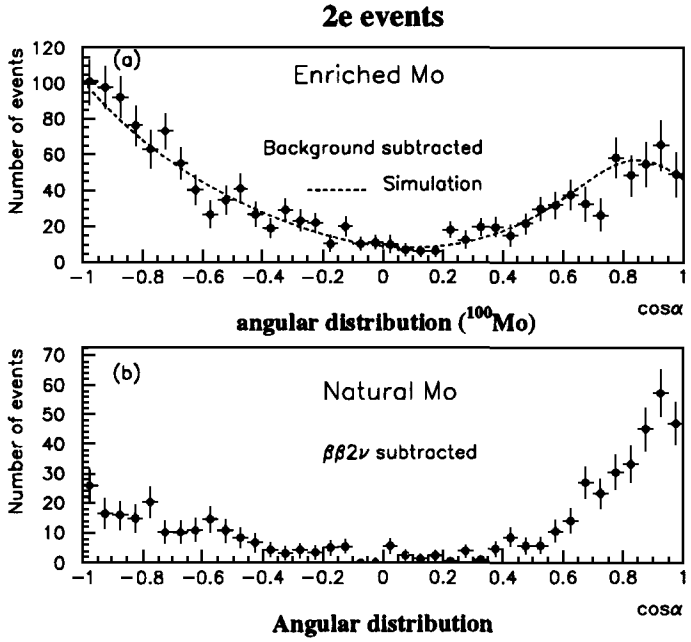

Fig. 3. Angular distributions for enriched and natural molybdenum.

Table 1. Half-life limits (90% C.L.). For each decay channel, an energy window, the corresponding number of experimental events, the number of background events including the external background and calculated $\beta\beta2\nu$ events, the efficiency, and the half-life limit are given ($\cos\alpha < 0.6$).

Isotope	^{100}Mo				^{116}Cd		
Channel (0ν-mode)	$0^+_{g.s.}$	Majoron	2^+_1	0^+_1	$0^+_{g.s.}$	Majoron	2^+_1
Window (MeV)	[2.6,3.0]	[2.1,2.9]	[2.1,2.5]	[1.4,1.9]	[2.4,3.0]	[1.8,2.55]	[1.2,1.5]
Number of events	1	31	30	290	1	11	52
Background + $\beta\beta2\nu$	2.	25.	22.5	306	3.2	12.2	54.
Efficiency (%)	3.6	1.4	2.4	2.7	3.7	1.8	1.8
$T_{1/2}$ (10^{21} y)	> 6.4	> 0.5	> 0.8	> 0.6	> 5.0	> 1.2	> 0.6

2.2 ^{100}Mo experiment

Figure 2 shows the $\beta\beta2\nu$ spectrum after background. In this experiment [4] the total running time was 6140 h. The 1 m^2 foil was divided into two parts. The first part was enriched molybdenum (98.4% ^{100}Mo) with a mass of 172 g and $\approx$40 μm thick, while the natural molybdenum (9.6% ^{100}Mo) part was 163 g and $\approx$44 μm thick. For both foils only limits on the activity of the most troublesome radioactive isotopes (^{214}Bi, ^{208}Tl and ^{234m}Pa) were obtained. So backgrounds from internal radioactivity were negligible. The solid line is a one-parameter fit of the spectrum, leading to the half-life

$$T^{2\nu}_{1/2} = [0.95 \pm 0.04(\text{stat}) \pm 0.09(\text{syst})] \times 10^{19}\text{y}\,.$$

From the same data, half-life limits on $\beta\beta0\nu$, $\beta\beta0\nu\text{M}^0$ decays and $\beta\beta0\nu$ transitions to excited states were obtained (Table 1).

Figure 3 shows the e-e angular ($\cos\alpha$) distributions on the enriched and natural molybdenum foils. The distribution of the angle between the two electrons in enriched molybdenum (background subtracted) is closely reproduced by $\beta\beta2\nu$ simulations and is quite different from the distribution extracted from the natural molybdenum data.

2.3 ^{116}Cd experiment

An earlier result drawn from 40% of the current data set was already published [5]. Here final results for 6588 h of data taking are presented. The source plane was again divided into two halves, the first one was a 152 g isotopically enriched cadmium foil (93.2% ^{116}Cd) 40 μm thick. The second half was a 143 g foil of natural cadmium (7.58% ^{116}Cd). Radioactive impurities in both foils were measured with HPGe detectors in the Fréjus Underground Laboratory. These measurements accord well with those extracted from NEMO-2 data, and the estimated background from ^{214}Bi, ^{208}Tl, ^{234m}Pa and the neutron flux is only a few 2e events in each foil and can be neglected after subtraction.

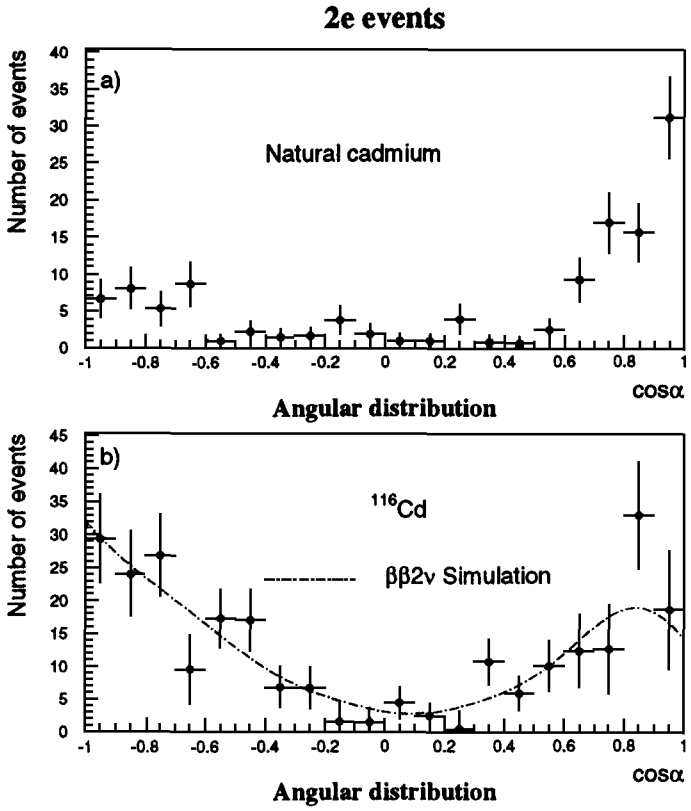

Fig. 4. Angular distributions in enriched and natural cadmium.

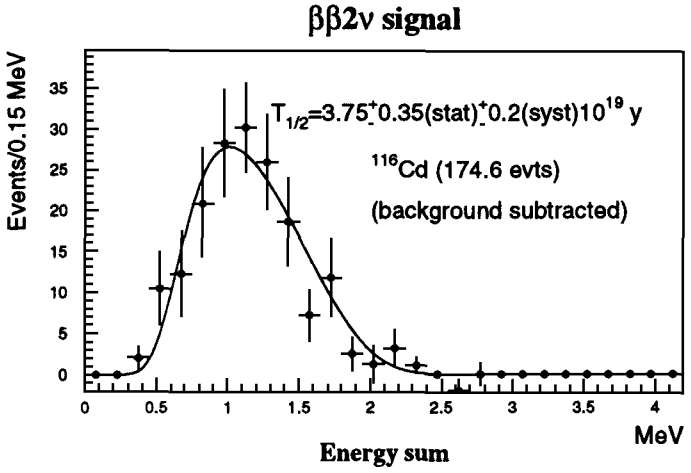

Fig. 5. Summed electron energy spectrum of $\beta\beta2\nu$ events in ^{116}Cd.

The $\cos\alpha$ distribution (Fig. 4) shows an external background peaked in the forward direction due to the external photon flux, so a $\cos\alpha < 0.6$ cut is applied. After background subtraction the $cos\alpha$ distribution is in agreement with the Monte Carlo simulated one (Fig. 4a).

In Fig. 5 the $\beta\beta$ energy spectrum in enriched cadmium (174.6 events) is shown after background subtraction (44.4 events). Using the calculated detection efficiency of the $\beta\beta2\nu$ decay of ^{116}Cd ($\varepsilon = 1.73\%$) one gets the half-life,

$$T_{1/2}^{2\nu} = [3.75 \pm 0.35(\text{stat}) \pm 0.21(\text{syst})] \times 10^{19}\text{y}\,.$$

Half-life limits on $\beta\beta0\nu$, $\beta\beta0\nu\text{M}^0$ decays and the $\beta\beta0\nu$ transition to the 2_1^+ excited state have been extracted from the data and are presented in Table 1. The energy windows, number of events, backgrounds, and efficiencies are also given.

2.4 ^{82}Se experiment

The source consists of two nearly symmetric halves. The first half contains 156.6 g of enriched selenium (97.02% is ^{82}Se) and the second part contains 137.7 g of natural selenium in which the ^{82}Se isotopic has an abundance of 8.73%. The sources were produced using a special technique to deposit selenium powder on thin films. The

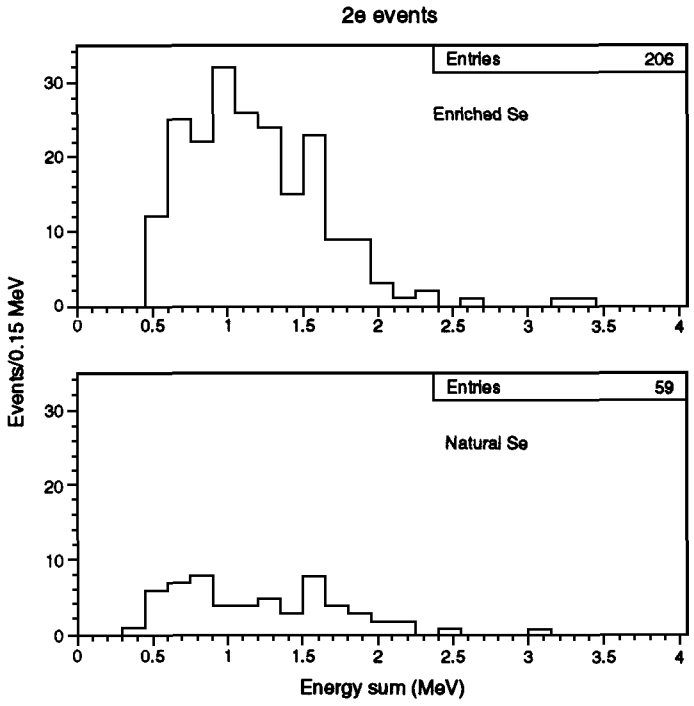

Fig. 6. Raw summed electron energy spectra in enriched (a) and in natural (b) selenium.

thickness of the foils is $\approx 50\,\mathrm{mg/cm^2}$ for enriched and $\approx 43\,\mathrm{mg/cm^2}$ for the natural ones.

Radioactive impurities in both foils have again been measured with HPGe detectors in the Fréjus Underground Laboratory before being placed in the NEMO-2 detector. The upper limits on contamination obtained in the enriched selenium for the three isotopes ^{214}Bi, ^{208}Tl and ^{234m}Pa are respectively 4.2, 2.5 and 33 mBq/kg, and in natural selenium these limits are 5, 2 and 16 mBq/kg, respectively. Some activity from ^{40}K was found in both samples, specifically 200 ± 30 mBq/kg in the enriched and 117 ± 16 mBq/kg in the natural selenium. The NEMO-2 detector was used by itself for purity control of the foils. A so-called "hot" points were discovered in the selenium foils, using $e\gamma$ and 2e channels. This "hot" points ($\approx 4.1\%$ of the natural selenium area and $\approx 0.9\%$ of the area in enriched selenium) were excluded from the analysis. Using the single electron energy spectra in the range [1.6–2.0] MeV, a limit on the difference of contamination in ^{234m}Pa in both foils of 4.3 mBq/kg is obtained which corresponds to less than 4.8 2e-events.

Presented here are preliminary results after 10357.5 h of data collection. Figure 6 shows the energy spectra of 2e-events in enriched and natural selenium foils (respectively 206 and 59 events). A $\cos\alpha < 0.6$ cut is applied. Taking into account mass difference of the natural and enriched foils and the contributions from ^{82}Se, ^{40}K and the chain connected with ^{208}Tl in the natural foil an "external" background in the enriched foil of 41.5 events is calculated. For "internal" backgrounds one can estimate that 16.5 events are contributed by ^{40}K. Consequently, the $\beta\beta$ signal is 148 events. Using the calculated detector efficiency for the $\beta\beta 2\nu$ decay for ^{82}Se ($\varepsilon = 1.28\%$) one gets,

$$T^{2\nu}_{1/2} = [0.8 \pm 0.1(\mathrm{stat}) \pm 0.1(\mathrm{syst})] \times 10^{20}\mathrm{y}\,.$$

This value is slightly different from the previous geochemical [6–8] and direct [9] experiment results. Half-life limits on the $\beta\beta 0\nu$ and $\beta\beta 0\nu \mathrm{M}^0$ processes in ^{82}Se were found to be 5×10^{21}y and 2×10^{21}y at the 90% CL.

2.5 ^{96}Zr experiment

The ^{96}Zr double beta decay measurements have been conducted in parallel with the selenium experiment. The source consists of two symmetric halves again and is located in the center of the source plane covering roughly 10% of the available area at the point of greatest geometric acceptance. The mass of the $^{96}ZrO_2$ and $^{nat}ZrO_2$ foils are 20.5 and 18.3 g, respectively. These foils were produced using a technology which binds the zirconium oxide with an organic film. The film thickness with some small variations is $50\,\mathrm{mg/cm^2}$ for enriched and $45\,\mathrm{mg/cm^2}$ for the natural sources. Enrichment of the Zr sample is 57.3% and thus the total mass of ^{96}Zr is 6.8 g.

Radioactive impurities in both foils have been measured with the HPGe detectors in the Fréjus Underground Laboratory before installation in the NEMO-2 detector. The upper limits on contamination obtained in the enriched Zr for the three isotopes ^{214}Bi, ^{208}Tl and ^{234m}Pa are respectively 12.5, 15 and 280 mBq/kg, and in natural Zr these limits are 13, 8 and 180 mBq/kg. Some activity from ^{40}K, ^{228}Ac, ^{154}Eu and

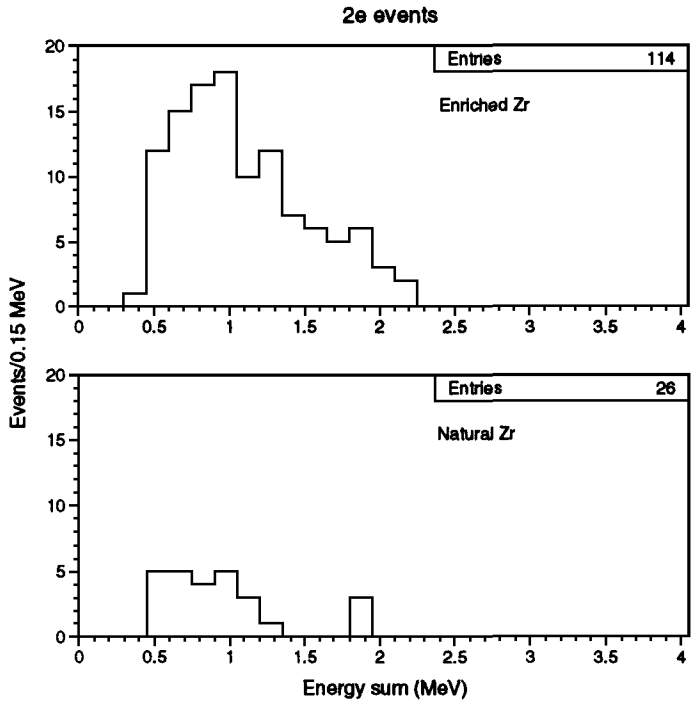

Fig. 7. Raw summed electron energy spectra in enriched and in natural zirconium.

^{152}Eu was observed in the enriched foil: 1080, 90, 50 and 66 mBq/kg respectively. In the natural foil only limits for these isotopes are observed: 200, 90, 50 and 66 mBq/kg respectively. Using the NEMO-2 purity control (eγ channel) a weak "hot" point in the enriched Zr foil ($\approx$ 6.8% of the area) was discovered and excluded from the analysis. Activities of 15$\pm$3.5 mBq/kg for ^{208}Tl and of 98$\pm$18 mBq/kg for ^{228}Ac in the enriched Zr foil were measured by NEMO-2.

Figure 7 shows the energy spectra of 2e-events in enriched and natural zirconium, 114 and 26 events after 10357.5 h. A $\cos\alpha < 0.6$ cut is applied. A large part of events in enriched Zr is connected with ^{228}Ac, ^{208}Tl, ^{40}K and others pollutions. Using the informations from HPGe and NEMO-2 measurements, the contributions of these isotopes can be estimated. This work is now in progress. In a "simple" analysis one can use the energy region greater than 1.5 MeV, where $\approx$ 34% of $\beta\beta2\nu$ events remain but internal and external backgrounds are strongly suppressed. Then 22 events in enriched and 3 events in natural Zr are observed. The contribution of the radioactive impurities to the enriched Zr spectrum is estimated to 3.9 events and 0.7 events to the natural Zr spectrum. As a result the positive effect is 15.8 events, that is corresponding to

$$T_{1/2} = [2.0\,^{+0.9(\mathrm{stat})}_{-0.5(\mathrm{stat})} \pm 0.5(\mathrm{syst})] \times 10^{19}\mathrm{y}\,.$$

Limits (90% CL) are obtained on $\beta\beta0\nu$ and $\beta\beta0\nu M^0$ decays, 8×10^{20} and 3×10^{20}, respectively.

3 NEMO-3 detector

In contrast to the ^{76}Ge experiments, the NEMO experiments [1] use tracking detectors which are not only able to measure the full energy released, but other parameters of the process such as the single electron energy, the angle between electrons, the coordinates of events, etc. The optimal operating parameters of the detector were investigated with the prototype NEMO-2 [3–5]. Currently the NEMO-3 detector is under construction and will be able to accommodate up to 10 kg of various double beta decay candidates (^{100}Mo, ^{116}Cd, ^{82}Se, ^{130}Te, ^{96}Zr, ^{150}Nd, etc). The lifetime limits after 5 years of measurement will be at the level 10^{25}y for $\beta\beta0\nu$ decay with $\langle m_\nu\rangle \approx (0.1\text{–}0.3)$eV, and $\approx 10^{23}$y for $\beta\beta0\nu M^0$ decay ($\langle g_{ee} > \approx 10^{-5}$), and finally $\approx 10^{22}$y for $\beta\beta2\nu$ decay.

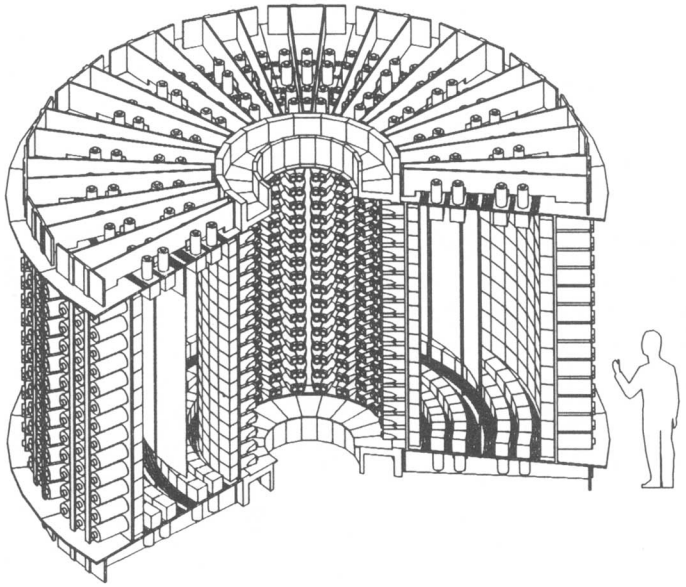

Fig. 8. Schematic view of the NEMO3 detector.

A general view of the detector's cylindrically symmetric geometry is shown in Fig. 8. The detector consists of a tracking volume filled with helium gas, a thin source foil divides the tracking volume vertically into two concentric cylinders with a calorimeter at the inner and outer most walls. The tracking system consists of 6000 Geiger cells 3 m long which are parallel to the detector's vertical axis. Energy and time-of-flight measurements are performed by the plastic scintillators covering

the two concentric surfaces discussed above and their associated end caps. The total number of low radioactive photomultipliers will approach 2000 and the weight of the scintillator will reach 7×10^3 kg. A magnetic field ($\approx$ 30 Gauss) will be used to reject backgrounds connected with pair creation and incoming electrons. A shield consisting of 20 cm of iron and 5 cm of lead will again protect the detector from external radioactivity.

4 Conclusion

The $\beta\beta2\nu$ decays of ^{100}Mo and ^{116}Cd have been investigated with high statistics and a favourable signal-to-background ratio ($\approx$ 3:1 for ^{100}Mo and $\approx$ 4:1 for ^{116}Cd). Also using the NEMO-2 detector the preliminary results for ^{82}Se and ^{96}Zr have been obtained. Following these measurements the NEMO-3 detector will replace NEMO-2 and an investigation of the neutrino masses to values as low as 0.1–0.3 eV will begin. This program will commence data collection in 1999.

References

[1] NEMO Collab.: Preprint LAL 94-29 (1994).

[2] D. Dassié et al.: Nucl. Inst. Meth. A **309** (1991) 465.

[3] R. Arnold et al.: Nucl. Inst. Meth. A **354** (1995) 338.

[4] D. Dassié et al.: Phys. Rev. D **51** (1995) 2090.

[5] R. Arnold et al.: JETP Lett. **61** (1995) 170.

[6] T. Kirsten: in *Proc. Int. Symp. "Nuclear Beta Decay and Neutrinos"*, Osaka (Japan) 1986 (Edited by T. Kotani, H. Ejiri and E. Takasugi), World Scientific, Singapore, 1986, p. 81.

[7] W.J. Lin et al.: Nucl. Phys. A **481** (1988) 477.

[8] O.K. Manuel: J. Phys. G **17** (1991) 221.

[9] S.R. Elliott et al.: Phys. Rev. C **46** (1992) 1535. 2452.